

# Efficient L1SPIRiT Reconstruction (ESPIRiT) for Highly Accelerated 3D Volumetric MRI with Parallel Imaging and Compressed Sensing

P. Lai<sup>1</sup>, M. Lustig<sup>2,3</sup>, A. C. Brau<sup>1</sup>, S. Vasanawala<sup>4</sup>, P. J. Beatty<sup>1</sup>, and M. Alley<sup>2</sup>

<sup>1</sup>Applied Science Laboratory, GE Healthcare, Menlo Park, CA, United States, <sup>2</sup>Electrical Engineering, Stanford University, Stanford, CA, United States, <sup>3</sup>Electrical Engineering and Computer Science, University of California, Berkeley, CA, United States, <sup>4</sup>Radiology, Stanford University, Stanford, CA, United States

## Introduction:

Highly accelerated data acquisition is demanded for 3D volumetric MRI. In recent years, many approaches<sup>[1,2,3]</sup> have been developed to integrate parallel imaging (PI) and compressed sensing (CS) to achieve higher acceleration than either method alone. Among such approaches, L<sub>1</sub>SPIRiT<sup>[3]</sup> synergistically combines PI and CS and has proven promising in clinical evaluations. However, this iterative solver is highly computationally intensive and poses difficulty for commonly available platforms. This work was aimed at developing an efficient L<sub>1</sub>SPIRiT scheme (ESPIRiT) to address this computation challenge.

## Theory:

L<sub>1</sub>SPIRiT is an iterative algorithm performing PI and CS operations serially in each iteration<sup>[3]</sup>. The PI operator resynthesizes k-space using a GRAPPA-like convolution kernel ( $G_k$ )<sup>[4]</sup>. This operation can be performed more efficiently with image-domain multiplications<sup>[5]</sup>:  $X_{n+1}(x,y) = X_n(x,y) \cdot G_I(x,y)$  (1), where  $X_{n,n+1}(x,y)$  are temporary image-domain solutions at pixel  $(x,y)$ ,  $G_I$  is image-domain unaliasing coil weights ( $G_I = F^{-1}(G_k)$ ). The CS operator transforms multi-coil images to sparse domain ( $w$ ) using wavelet ( $\Psi$ ) and pursues  $\min \|w\|_1$  using softthresholding ( $T$ ). The computation of the PI and CS operators is  $O(N_x N_c^2 N_{it})$  and  $O(N_x N_c N_{it})$ , respectively, where  $N_x$ ,  $N_c$  and  $N_{it}$  are the numbers of pixels to reconstruct, coil channels and iterations in the entire reconstruction, respectively. This work intended to reduce computation from the following three perspectives:

**1. modified L<sub>1</sub>SPIRiT to remove  $N_c$ :** The PI operator utilizes k-space correlations and ideally should converge to the “truth” image:  $X = M \cdot C$ , where  $M$  and  $C$  represent spin density and coil sensitivity distributions, respectively. By rewriting equation (1) ( $(x,y)$  omitted below for simplicity), we have  $M \cdot C = M \cdot C \cdot G_I$  (2). By eliminating the common scalar  $M$  in (2), we get  $C = C \cdot G_I$  (3), which means  $C$  (size:  $N_c \times 1$ ) corresponds to the eigenvector of  $G_I$  (size:  $N_c \times N_c$ ) with eigenvalue=1 at each pixel. (3) offers an approach to estimate  $C$  from  $G_I$  (Fig. 1A), with which we perform PI & CS in an alternative way. Our PI operator pursues a new solution that is consistent with coil weighting and meanwhile is L<sub>2</sub>-closest to the previous solution:  $\min \|X_{n+1} - X_n\|_2$ , s.t.  $X_{n+1} = M \cdot C$ . The derived optimal solution is:  $X_{n+1} = C^{H*} \cdot X_n \cdot C / \|C\|_2^2$  (4). Let  $C_s = C / \|C\|_2$ , we can rewrite and split (4) to two operators:  $S_I: M_{n+1} = C_s^{H*} \cdot X_n$  and  $S_2: X_{n+1} = M_{n+1} \cdot C_s$ .  $S_{I/2}$  reduces the matrix operation ( $O(N_c^2)$ ) in (1) to much faster vector operation ( $O(N_c)$ ). Furthermore, an intermediate magnetization image  $M_{n+1}$  is produced such that CS can now be performed in the coil-combined image pursuing joint sparsity rather than coil by coil. This further reduces the computation of the CS operator by  $N_c \times$ . Additionally, (3) is well-conditioned only at pixels with signals, while in air, (3) produces eigenvalues largely different from 1 (Fig. 1A). Thus, the eigenvalue map of  $G_I$  can be used to generate an image support ( $I_S$ ) that can eliminate artifacts in air and improve the conditioning of L<sub>1</sub>SPIRiT<sup>[6]</sup>.

**2. pixel-specific convergence to reduce  $N_x$ :** It is observed that L<sub>1</sub>SPIRiT convergence is highly pixel-specific (Fig. 2). For most pixels, only a small number of iterations are needed. Taking advantage of this feature, converged pixels can be “checked out” and excluded in later iterations. This can rapidly reduce  $N_x$  remaining in reconstruction (Fig. 2), which can accelerate  $S_{I/2}$  operators and Fourier and wavelet transforms performed on an increasingly sparser image.

**3. PI initialization to reduce  $N_{it}$ :** It has been shown that PI can improve the initial condition for L<sub>1</sub>SPIRiT than conventionally used zero-filling and therefore reduce  $N_{it}$  needed<sup>[7]</sup>. Accordingly, Poisson-disk k-space sampling (PDS) is replaced by tiled-PDS (tPDS) for efficient PI initialization without sacrificing image quality<sup>[7]</sup>.

## Methods:

Based on the above theory, we proposed ESPIRiT with improved efficiency. As illustrated in Fig. 1, ESPIRiT consists of: **A.** calculating  $C$  and  $I_S$ , **B.** PI initialization and **C.** modified L<sub>1</sub>SPIRiT. Step **A**: 1) calculates  $G_k$  (kernel size:  $7 \times 7 \times 7$ ) using calibration signals in the center portion of the sampled k-space ( $x_0$ ); 2) calculates low-resolution  $G_I$  ( $60 \times 60 \times 60$ ) from  $G_k$ ; 3) calculates the eigenvector of matrix  $G_I$  at each pixel with eigenvalue closest to 1; next interpolates the eigenvalue and eigenvector maps to full resolution and derive 4) image support ( $I_S$ ) and 5) coil maps ( $C$ ). Step **C** iteratively performs: i)  $S_I$ : combine coil images  $X$  to a magnetization image  $M$ ; ii) CS on  $M$ ; iii) suppress signals in air based on  $I_S$ ; iv) calculate  $\Delta M = \|M_{n+1} - M_n\|_2$  and checkout converged pixels with sufficiently small  $\Delta M$ ; v)  $S_2$ : reproduce coil images  $X$ ; vi) set acquired k-space data to  $x_0$ .

To evaluate ESPIRiT, we scanned 2 volunteers (1 brain & 1 knee) on GE 1.5T with 8-channel coils using a 3D fast spin echo Cube sequence. Imaging parameters were selected to generate proton density weighting on the knee and T<sub>2</sub> weighting on the brain. Full k-space was acquired and offline decimated to simulate 1) PDS and 2) tPDS with  $2.5 \times 2.5$  acceleration (net:  $5.4 \times$ ). The PDS and tPDS datasets were processed in Matlab using L<sub>1</sub>SPIRiT with  $N_{it}=50$  and ESPIRiT with  $N_{it}=25$ , respectively.

## Results:

Fig. 3 shows the results on the knee. ESPIRiT (b) produces image quality very similar to the full k-space reconstruction (a), while L<sub>1</sub>SPIRiT (c) generates considerable errors (arrows). The difference can be better appreciated in the zoomed-in figures (d-f). The error level of ESPIRiT (g) is visually lower than that of L<sub>1</sub>SPIRiT (h). Similar results were observed on the brain dataset. The RMES’s are L<sub>1</sub>SPIRiT: 7.83%/14.19% (knee/brain) and ESPIRiT: 6.99%/11.77%. ESPIRiT ran  $\sim 10 \times$  faster than L<sub>1</sub>SPIRiT. (note: higher acceleration in computation compared to L<sub>1</sub>SPIRiT is anticipated in a C implementation, which can better leverage pixel-specific convergence).

## Discussions:

ESPIRiT can significantly improve the computation efficiency of L<sub>1</sub>SPIRiT, by reducing the computation complexity ( $\sim N_c \times$ ), number of pixels to process (on average  $\sim 2 \times$ ) and number of iterations needed for convergence ( $\sim 2 \times$ ). The sensitivity maps in ESPIRiT are derived from k-space correlations and should be relatively insensitive to difficulties in explicit sensitivity estimation<sup>[8]</sup>. Our initial results show that ESPIRiT can also achieve slightly more accurate reconstructions within half the number of iterations compared to L<sub>1</sub>SPIRiT.

**References:** [1] King, ISMRM 2008:1488; [2] Liu, ISMRM 2008:3154; [3] Lustig ISMRM, 2009:334; [4] Lustig, ISMRM 2007:333; [5] Brau, MRM, 2008, 59:382; [6] Klaas, MRM 1999, 42:952; [7] Lai, ISMRM Parallel Imaging Workshop, 2009; [8] Griswold, MRM 2004, 52:1118

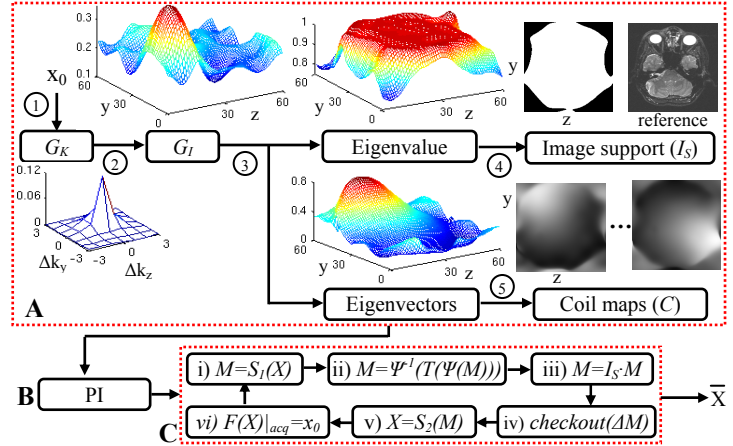


Fig.1 Flow chart of ESPIRiT reconstruction

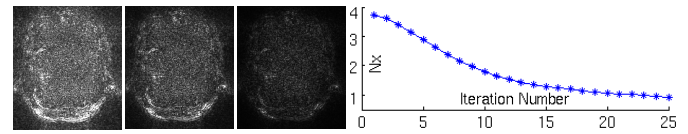


Fig.2 Difference produced by L<sub>1</sub>SPIRiT in iteration 5 (1st), 10 (2nd) & 25 (3rd). Reduction of  $N_x (\times 10^4)$  over ESPIRiT iterations (4th).

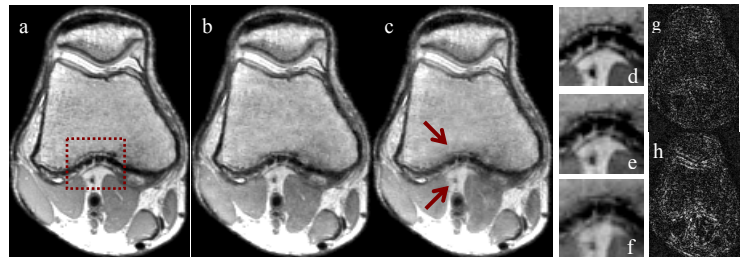


Fig.3 Reconstruction using a) full k-space, b) ESPIRiT, c) L<sub>1</sub>SPIRiT. d-f show a zoomed-in area (dotted in a) for a-c. g & h are error images for b & c, respectively